Transient Cooling of a Square Region of Radiating Medium

Robert Siegel
NASA Lewis Research Center, Cleveland, Ohio 44135

A time-accurate numerical solution was carried out for transient radiative cooling of a gray emitting and absorbing medium in a square two-dimensional region. The integro-differential energy equation for transient temperature distributions was solved in two stages. At each time increment, the local radiative source term was obtained by numerical integration of the temperature field using two-dimensional Gaussian integration over rectangular subregions. Then the differential portion of the equation was integrated forward in time by use of the local first and second time derivatives. The results were compared with available limiting cases, and excellent agreement was obtained. Transient results are given for a wide range of optical thicknesses of the region. Optimum transient cooling is obtained when the optical side length is about 4.

Nomenclature

A_R = aspect ratio of rectangular region, d/b
a = absorption coefficient of radiating medium, 1/m
B_0 = optical length of short side of rectangle, ab
b = length of short side of rectangle, m
c_p = specific heat of radiating medium, J/(kg – K)
d = length of long side of rectangle, m
Q = heat loss from entire perimeter for a unit of axial length z, W
$\tilde{Q}$ = dimensionless heat loss, $Q/2(b+d)\sigma T_i^4$
q_ℓ, q_s = local heat fluxes leaving long and short sides, W/m^2
r = distance between two locations in medium, m; $R = r/b$
S_n = function defined in Eq. (3)
T = absolute temperature, K; $\tilde{T} = T/T_i$
T_i = initial uniform temperature, K
T_m = integrated instantaneous mean temperature of medium, K; $\tilde{T}_m = T_m/T_i$
x,y,z = rectangular coordinates, m; $X = x/b$, $Y = y/b$, $Z = z/b$
ϵ_m = transient emittance based on instantaneous Q and T_m
ϵ_{ut} = emittance for region at uniform temperature
θ = angular coordinate
ξ = argument in Eq. (3)
ρ = density of radiating medium, kg/m^3
σ = Stefan-Boltzmann constant, W/(m^{2}K^4)
τ = time, s; $\tilde{\tau} = (4\sigma T_i^3/\rho c_p b)\tau$

Introduction

BEGINNING in the early 1980s, the solutions involving radiative transfer in absorbing and emitting media with nonuniform temperature distributions have advanced from primarily one-dimensional geometries to two- and some three-dimensional situations. Numerical solutions of these more difficult multidimensional cases have become feasible as larger and faster computers became available. In addition to accounting for geometric complexity, another variable in some instances is time. A transient situation adds considerably to the computational effort, since at each time step, the multidimensional calculations must be performed as in an entire steady problem. Transient solutions will be obtained in this paper for a two-dimensional radiative transfer problem.

Greater computational speed has also expanded the methods that are feasible for obtaining solutions. Direct methods of numerical integration can now be implemented to augment the various more analytical approximate expansion methods that were developed in the past. The numerical integrations have been carried out by use of discrete ordinates (angular integration subregions about each location),[1,2] finite elements,[3,4] and Gaussian integration in rectangular subregions of the geometry.[5] Some examples of analyses for rectangular geometries by use of other methods are in Refs. 6-9. The previous work has been primarily for steady-state conditions. Situations were analyzed, such as rectangular regions having three cool boundaries at the same uniform temperature and one boundary at an elevated uniform temperature; this is a condition of radiative equilibrium.[6] Another example is radiation from a rectangle with uniform heat generation in the medium.[7]

The transient problem considered here has application to radiative cooling of high-temperature media, such as porous ceramic insulating materials, and to the energy that can be dissipated by proposed radiators of the particle or liquid-drop type for elimination of waste heat in outer space applications. The analysis is developed for a radiating medium of rectangular shape, and numerical results are provided for a square geometry. The radiating medium is initially at uniform temperature and is then placed into low-temperature black surroundings. If the region is optically thin, radiation leaves directly from throughout the entire volume, and the entire region decreases in temperature rather uniformly with time. For an optically thick square region, the outer portions begin to cool rapidly, especially near the corners. The temperature distribution along the boundary becomes quite nonuniform, with the lowest values at the corners. The emittance of the region begins to deviate significantly from that for a region at uniform temperature. The emittance, based on using the instantaneous integrated mean temperature as the characteristic temperature, decreases while the transient temperature distribution is developing. For the cooling conditions of cold black surroundings considered here, the emittance approaches a steady value that depends on the optical dimension of the region. This behavior has been shown by the analysis in Ref. 5. It is found here that the steady value of the emittance is reached for each optical thickness after about 25% of the initial energy has been radiated away.

In Ref. 5, the fully developed solution where the emittance becomes constant with time was obtained by a separation of variables solution, and results were compared with the limiting conditions of a region cooling at uniform temperature. The present study continues the investigation of Ref. 5 by obtain-

Received Dec. 15, 1989; revision received Feb. 28, 1990; accepted for publication March 2, 1990.

*Senior Research Scientist. Office of the Chief Scientist, Mail Stop 5-9. Fellow AIAA.

ing transient solutions throughout the entire cooling process. The limiting results[5] showed that for an optically thin region there is only a small range between the maximum (uniform temperature) and minimum (fully developed transient) emittance. Hence, there is not much to be gained by studying the details throughout the transient. For moderate and large optical thicknesses, there is a significant decrease in emittance, especially early in the transient. For large optical thicknesses, there are large transient temperature decreases near the boundaries. The temperature distributions must be obtained very accurately as they govern the transient heat loss. As discussed in Ref. 8, diffusion types of approximations often yield inaccurate temperature distributions; this is especially true near boundaries. The present numerical integration method provides accurate temperature distribution solutions of the energy equation and hence accurate transient cooling results.

Analysis

Energy Equation for Radiative Cooling

A two-dimensional rectangular region, as shown in Fig. 1, consists of a gray emitting and absorbing medium initially at uniform temperature. The region is placed into black surroundings at a much lower temperature, and transient cooling occurs by radiative heat loss. Heat conduction is assumed to be small relative to radiative transfer. The geometry is long enough in the z direction so that the transient temperature distributions depend only on x,y and τ. The energy equation has been derived in the literature, such as in Refs. 5 and 6. The local decrease of internal energy within the medium is produced by the local net radiative loss. The net radiative loss is the result of local volume emission, $4a\sigma T^4(x,y,\tau)$, minus the local reabsorption of energy that arrives from all of the surrounding volume. This balance yields the transient energy equation for constant properties,

$$-\rho c_p \frac{\partial T}{\partial \tau} = 4a\sigma T^4(x,y,\tau) - a^2\sigma \int_{x'=0}^{d}\int_{y'=0}^{b} T^4(x',y',\tau) \times \frac{S_1(ar)}{r}\,dx'\,dy' \tag{1}$$

where $r^2 = (x'-x)^2 + (y'-y)^2$. This is a nonlinear integro-differential equation for the transient temperature distribution and has the dimensionless form

$$-\frac{\partial \tilde{T}}{\partial \tilde{\tau}} = B_0\tilde{T}^4(X,Y,\tilde{\tau}) - \frac{B_0^2}{4}\int_{X'=0}^{A_R}\int_{Y'=0}^{1} \tilde{T}^4(X',Y',\tilde{\tau}) \times \frac{S_1(B_0R)}{R(X,Y,X',Y')}\,dX'\,dY' \tag{2}$$

where $R(X,Y,X',Y') = [(X'-X)^2 + (Y'-Y)^2]^{1/2}$. The S_1 is one of the class of S_n functions examined in Ref. 10 that arise in two-dimensional radiative transfer,

$$S_n(\xi) = \frac{2}{\pi}\int_0^{\pi/2} e^{-\xi/\cos\theta}\cos^{n-1}\theta\,d\theta \tag{3}$$

As will be described, the solution for $\tilde{T}(X,Y,\tilde{\tau})$ from Eq. (2) was obtained by a direct numerical integration in X,Y and by a forward integration in $\tilde{\tau}$. Before presenting the numerical method, some relations are given for boundary heat fluxes and average emittances.

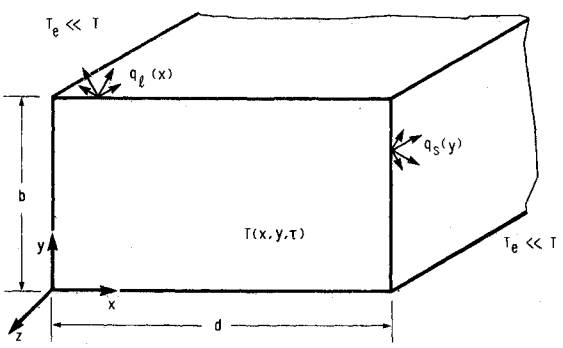

Fig. 1 Cross section of two-dimensional radiating rectangular region (dimension is large in z direction).

Local Heat Fluxes Leaving the Boundary and Emittance Relations

The local heat flux along the boundary is obtained by integrating over the volume the energy that arrives from each volume element. This was done in Ref. 5 to provide the fluxes leaving the short and long sides in Fig. 1 as

$$\frac{q_s(Y,\tilde{\tau})}{\sigma T_i^4} = B_0\int_{X'=0}^{A_R}\int_{Y'=0}^{1} \tilde{T}^4(X',Y',\tilde{\tau})(A_R - X') \times \frac{S_2(B_0R_1)}{R_1^2}\,dY'\,dX' \tag{4a}$$

$$\frac{q_\ell(X,\tilde{\tau})}{\sigma T_i^4} = B_0\int_{X'=0}^{A_R}\int_{Y'=0}^{1} \tilde{T}^4(X',Y',\tilde{\tau})(1 - Y') \times \frac{S_2(B_0R_2)}{R_2^2}\,dY'\,dX' \tag{4b}$$

where $R_1^2 = (A_R - X')^2 + (Y - Y')^2$, $R_2^2 = (X - X')^2 + (1 - Y')^2$.

The energy leaving instantaneously from the entire boundary is found by integrating the local fluxes over the four sides to yield

$$Q(\tau) = 2\left[\int_0^d q_\ell(x,\tau)\,dx + \int_0^b q_s(y,\tau)\,dy\right]$$

This has the dimensionless form

$$\frac{Q(\tau)}{2(b+d)\sigma T_i^4} = \tilde{Q}(\tilde{\tau}) = \frac{1}{1+A_R}\left[\int_0^1 \tilde{q}_s(Y,\tilde{\tau})\,dY + \int_0^{A_R}\tilde{q}_\ell(X,\tilde{\tau})\,dX\right] \tag{5}$$

At any time during transient cooling, the mean temperature is obtained from $T(x,y,\tau)$ by using

$$T_m(\tau) = (1/bd)\int_{x=0}^{d}\int_{y=0}^{b} T(x,y,\tau)\,dx\,dy$$

which gives the dimensionless form

$$\frac{T_m(\tau)}{T_i} = \tilde{T}_m(\tilde{\tau}) = \frac{1}{A_R}\int_{X=0}^{A_R}\int_{Y=0}^{1} \tilde{T}(X,Y,\tilde{\tau})\,dX\,dY \tag{6}$$

The instantaneous emittance for the entire region, based on the mean temperature, is found from the heat balance, $Q(\tau) = 2(b+d)\epsilon_m(\tau)\sigma T_m^4(\tau)$. In dimensionless form, this gives

$$\epsilon_m(\tilde{\tau}) = \tilde{Q}(\tilde{\tau})/\tilde{T}_m^4(\tilde{\tau}) \tag{7}$$

As a check on the numerical work, the $\epsilon_m(\tilde{\tau})$ can also be obtained from the heat balance, $2(b+d)\epsilon_m(\tau)\sigma T_m^4(\tau) = -\rho c_p bd\,dT_m(\tau)/d\tau$. This has the dimensionless form

$$\epsilon_m(\tilde{\tau}) = -\frac{2A_R}{1+A_R}\frac{1}{\tilde{T}_m^4}\frac{d\tilde{T}_m}{d\tilde{\tau}} \tag{8}$$

If $\epsilon_m(\tilde{\tau})$ is changing slowly with time, Eq. (8) can be integrated

analytically over a small time interval (integrate from $\tilde{\tau}$ to $\tilde{\tau} + \Delta\tilde{\tau}$) to yield the relation

$$\epsilon_m(\tilde{\tau} \text{ to } \tilde{\tau} + \Delta\tilde{\tau}) = \frac{2A_R}{1 + A_R} \frac{1}{3\Delta\tilde{\tau}} \left[\frac{1}{T_m^3(\tilde{\tau} + \Delta\tilde{\tau})} - \frac{1}{T_m^3(\tilde{\tau})} \right] \quad (9)$$

This provides another equality to check the consistency of results from the numerical solution.

For comparison, transient solution results are obtained for a region that always has a spatially uniform temperature. For this situation, the emissivity is a constant for each optical dimension B_0. It is called ϵ_{ut} and is found at the beginning of each transient solution where the first set of boundary heat flux integrations is for the initial condition of uniform temperature. The ϵ_{ut} is also given in Ref. 11 as obtained by another method. By integrating Eq. (8) with $\epsilon_m = \epsilon_{ut}$,

$$\tilde{T}_m(\tilde{\tau}) = [1 + 3\epsilon_{ut}\tilde{\tau}(1 + A_R)/2A_R]^{-1/3} \quad (10)$$

Then from $Q(\tau) = 2(b + d)\epsilon_{ut}\sigma T_m^4(\tau)$, the instantaneous heat loss can be expressed in terms of ϵ_{ut} and τ as

$$\frac{Q(\tilde{\tau})}{2(b + d)\sigma T_i^4} = \frac{\epsilon_{ut}}{[3\tilde{\tau}\epsilon_{ut}(1 + A_R)/2A_R + 1]^{4/3}} \quad (11)$$

Numerical Solution of Integro-Differential Equation

The method for forward integration in time of Eq. (2) will be developed first. Then the method of evaluating the double integral on the right-hand side will be given. Letting the right-hand side be called $RHS(\tilde{T}, \tilde{\tau})$, Eq. (2) is written as

$$-\frac{\partial \tilde{T}}{\partial \tilde{\tau}} = RHS(\tilde{T}, \tilde{\tau}) \quad (12)$$

Let $\tilde{T}(X, Y, \tilde{\tau})$ and $\tilde{T}(X, Y, \tilde{\tau} + \Delta\tilde{\tau})$ be written as $\tilde{T}_n(X, Y)$ and $\tilde{T}_{n+1}(X, Y)$. For each X, Y location,

$$\tilde{T}_{n+1} - \tilde{T}_n = -\int_{\tilde{\tau}}^{\tilde{\tau} + \Delta\tilde{\tau}} RHS(\tilde{\tau})\, d\tilde{\tau} \quad (13)$$

This integral is approximated by the trapezoidal rule as

$$\tilde{T}_{n+1} - \tilde{T}_n = -\frac{\Delta\tilde{\tau}}{2}(RHS_{n+1} + RHS_n) \quad (14)$$

The value of RHS_{n+1} is obtained by using the expansion

$$RHS_{n+1} = RHS_n + \left.\frac{\partial(RHS)}{\partial \tilde{T}}\right|_n (\tilde{T}_{n+1} - \tilde{T}_n) \quad (15)$$

This is substituted into Eq. (14) to give

$$\tilde{T}_{n+1} - \tilde{T}_n = -\frac{\Delta\tilde{\tau}}{2}\left[2RHS_n + \left.\frac{\partial(RHS)}{\partial T}\right|_n (\tilde{T}_{n+1} - \tilde{T}_n) \right]$$

Solving for $\tilde{T}_{n+1}$, this yields

$$\tilde{T}_{n+1} = \tilde{T}_n - \frac{\Delta\tilde{\tau}\, RHS_n}{1 + (\Delta\tilde{\tau}/2)[\partial(RHS)/\partial\tilde{T}]|_n} \quad (16)$$

The derivative of the RHS is obtained from Eq. (2) as,

$$\frac{\partial(RHS)}{\partial \tilde{T}} = 4B_0\tilde{T}^3(X, Y, \tilde{\tau}) - B_0^2 \int_{X'=0}^{A_R} \int_{Y'=0}^{1} \tilde{T}^3(X', Y', \tilde{\tau}) \times \frac{S_1(B_0R)}{R(X, Y, X', Y')}\, dX'\, dY' \quad (17)$$

To move ahead in time by use of Eq. (16), the double integrals in Eqs. (2) and (17) must be evaluated at each X, Y (the integration variables are X', Y'). The numerical integration method is now discussed.

Since the function $S_1(B_0R)$ is well behaved as $R \to 0$, the integrands of Eqs. (2) and (17) appear to be singular, because of the $1/R$ factor, when the integration variables X', Y' approach the grid point X, Y. The integrands are not singular, since by using cylindrical coordinates R, θ about the location X, Y, the $dX\, dY$ becomes $R\, dR\, d\theta$ and the $1/R$ is removed. However, when using rectangular coordinates for purposes of integration, the apparent singularity must be dealt with for small R. For this reason, the integration about each grid point X, Y was divided into seven regions, as shown in Fig. 2a. Region 7 is a small square with a width less than one-half of a grid spacing. This was replaced by a small circle having the same area as the square and the integration for region 7 carried out in cylindrical coordinates. The contribution by this region was a small part of the total double integral, so this approximation did not yield significant error.

To carry out the integrations, the entire rectangular cross section was covered with a square grid of equally spaced points. For the integrations at each $\tilde{\tau}$, two-dimensional spline fits were made of $\tilde{T}^4(X, Y, \tilde{\tau})$ and $\tilde{T}^3(X, Y, \tilde{\tau})$ using IMSL routines BSNAK and BS2IN. The spline coefficients were used to interpolate values at locations between the grid points, as called for by the two-dimensional integration subroutines. To check the calculations, two different subroutines were used, both employing Gaussian integration. One was IMSL routine QAND, which inserts additional integration points, for a total of up to 256 in each coordinate direction, to try to evaluate the integral within a given error. The other Gaussian routine, SQUAD1, was developed at NASA Lewis Research Center and is described in Ref. 12. This routine uses 16 Gaussian points in each direction. Sample cases from the two routines were found to be in excellent agreement. The SQUAD1 routine provided significantly shorter computation times and was used for most of the transient cases.

The results given here are for a square geometry. The number of fixed grid points used across the side length depended on the optical dimension B_0. For small B_0, such as $B_0 = 1$, the temperature profiles are fairly flat, and 11 grid points in each direction were sufficient. A larger number of points changed the results by less than 0.5%. For $B_0 = 15$, the number of points in each direction was increased to 25 because of the large curvature in the temperature profiles. This made the

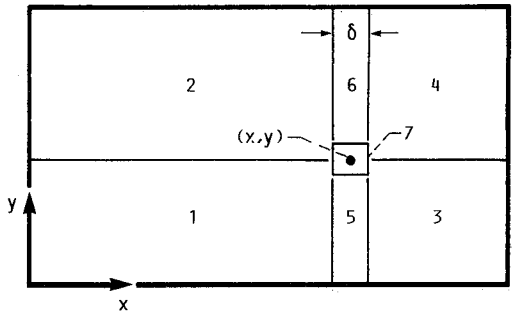

a) Regions for double integration in energy equation

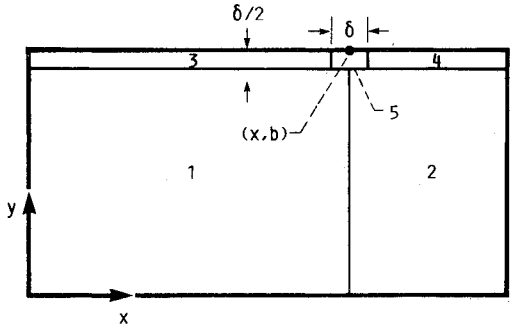

b) Regions for double integration in surface flux $q_y(x, \tau)$

Fig. 2 Integration regions used for computing energy and heat flux relations.

computation time longer for the larger B_0 cases. Most of the calculations were done with 21 points. The calculations were carried out with a CRAY X-MP computer and required about 30 s per time increment for an 11-point grid, and 2 min per time increment for a 25-point grid. About 15–20 time increments were required to go from an initial dimensionless temperature of unity to a final dimensionless mean temperature of 0.65 (the region has radiated away 35% of its initial energy). A variable size for the time increment was used because the cooling rate decreases substantially as the mean temperature decreases. A small time increment, such as $\Delta\tilde{\tau} = 0.01$, was used initially, and the change in $\tilde{T}_m$ per time increment was noted. If $\Delta\tilde{T}_m$ was smaller than a specified amount, such as 0.03, the $\Delta\tilde{\tau}$ was increased by a small amount such as 0.01. Thus, as the calculation proceeded forward in time, the $\Delta\tilde{\tau}$ was increasing to keep $\tilde{T}_m$ changing at a steady rate. For smaller mean temperatures, the solution can be continued analytically. This is possible because the transient emissivity of a rectangle, based on the instantaneous mean temperature, reaches a constant value for each set of parameters, as shown in Ref. 5, and the dimensionless temperature profile reaches a fixed shape.

A similar spatial integration procedure was used to determine the local heat fluxes along the boundary. Five integration subregions were used, as shown in Fig. 2b. To evaluate Eq. (4), the $S_2(B_0R)$ values are required, and similarly $S_1(B_0R)$ values were needed for Eqs. (2) and (17). These functions were evaluated from Eq. (3) by using the IMSL integration routine QAND, and tables of values were prepared. Values called for by the two-dimensional integration routine were interpolated by using IMSL cubic spline interpolation routines CSINT and CSVAL.

Results and Discussion

Typical transient temperature distributions are shown in Fig. 3. The initial temperature distribution is uniform, and the transient is caused by sudden exposure to cold black surroundings. As expected from various steady-state radiative transfer solutions in the literature, the temperature profiles are quite dependent on the optical length of the side of the square region. Figure 3 gives profiles for three optical thicknesses and for three times during the transient, corresponding to when about 10, 20, and 33% of the initial energy has been radiated away. For each time, two profiles are shown, one along the centerline $Y = 0.5$ and the second along the boundary $Y = 1$. From symmetry, only one-half of each profile need be shown ($0 \le X \le 0.5$).

The dimensionless temperatures are initially unity. As would be expected, the transient profiles do not become highly curved when B_0 is small (optically thin region). For $B_0 = 2$ (Fig. 3a), the temperature distributions along the boundary remain fairly flat. The centerline temperatures decrease somewhat more slowly with time and are a little more curved. For a large B_0, such as $B_0 = 15$, there can persist, after the onset of the transient, a relatively uniform temperature region in the

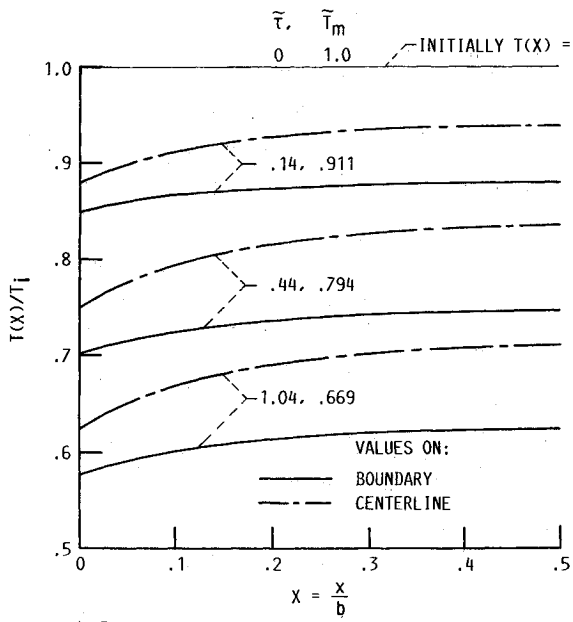

a) Optical dimension $B_0 = 2$

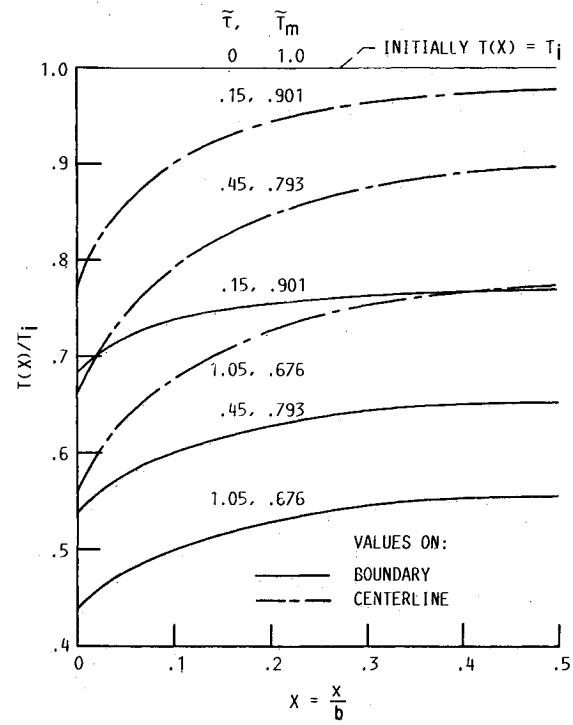

b) Optical dimension $B_0 = 7$

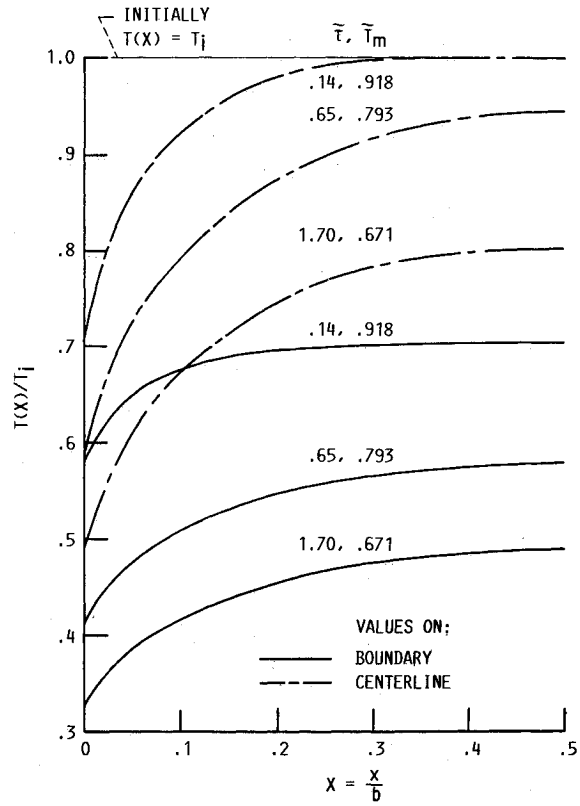

c) Optical dimension $B_0 = 15$

Fig. 3 Transient temperature distributions along boundary and centerline for a square radiating region.

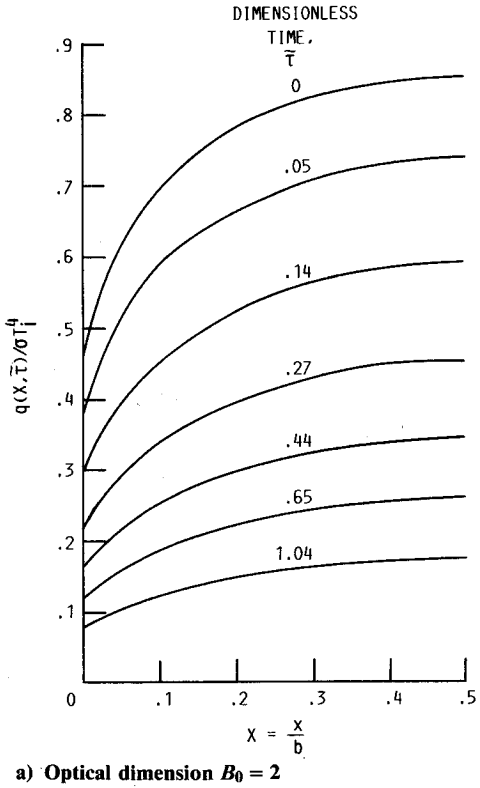

a) Optical dimension $B_0 = 2$

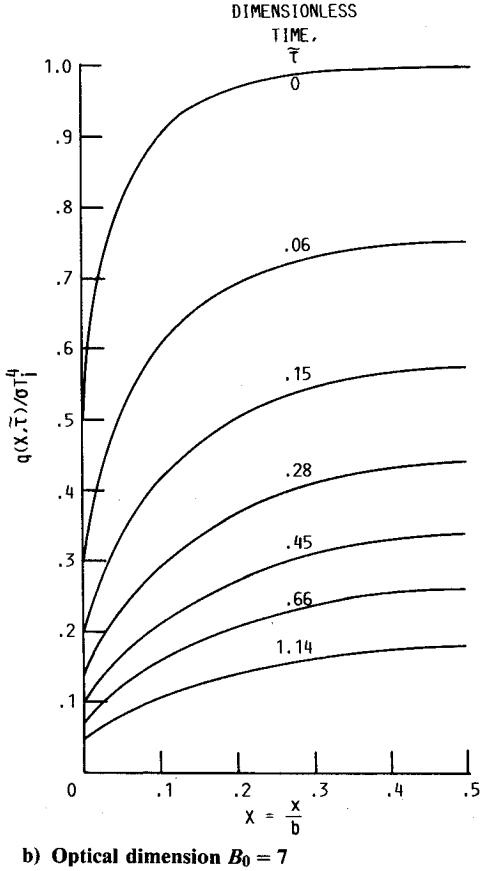

b) Optical dimension $B_0 = 7$

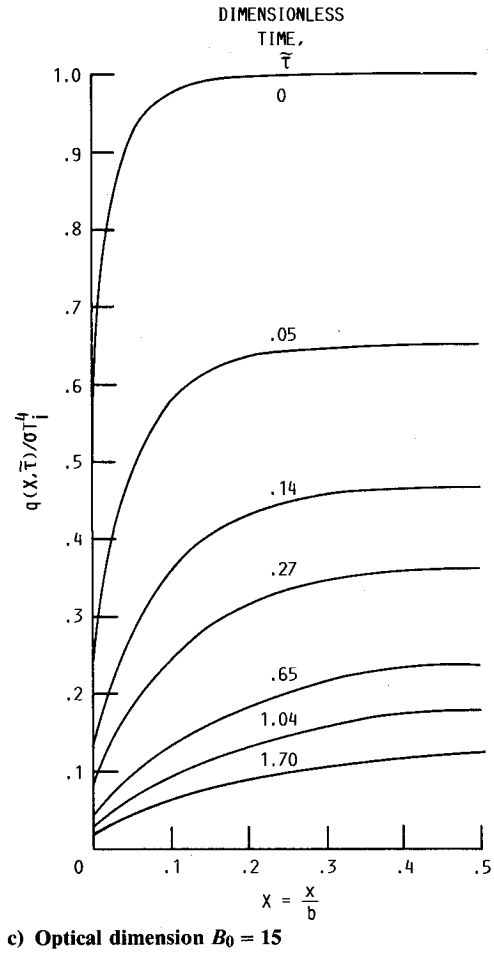

c) Optical dimension $B_0 = 15$

Fig. 4 Transient local heat flux distribution along the boundary of a square radiating region.

central portion of the medium, because the radiative energy has difficulty propagating out from the region interior. In contrast, the corner temperatures decrease rapidly after cooling begins. In this rather optically thick medium ($B_0 = 15$), the central portion of the volume cools much more slowly than the portion near the boundaries.

Figure 4 gives the heat flux that a square region of radiating medium radiates locally along its boundary. The figure has three parts for the same B_0 values as in Fig. 3. The smallest fluxes are always at the corners. The largest fluxes are at the center of the side where radiant energy arrives from more directions than at the corner. Consider first the initial condition when the radiating medium is at uniform temperature. The radiated flux at the boundary varies considerably with location; this is also shown by the analytical solution in Ref. 11. The present numerical results agreed within 0.5% accuracy

with the analytical solution. For large B_0, the dimensionless flux at the corner is ½, while that at the center of the side is 1 (blackbody radiation).

After transient cooling begins, for large B_0 there is a very rapid decrease in boundary flux at early times. This is because radiation from the interior of the region has difficulty penetrating to the outside because of reabsorption within the optically thick medium. This causes the temperatures adjacent to the boundary to decrease substantially, and the fluxes at the boundary decrease rapidly. This is also the transient behavior of the heat loss from the entire region, as shown for $B_0 = 15$ in Fig. 5.

The heat loss from the entire region is obtained by integrating the heat losses around the boundary or by using the change in instantaneous integrated mean temperature. The ordinate in Fig. 5 is the transient heat loss relative to that radiated by a black square region at the uniform initial temperature. The uppermost curve on the figure, shown for comparison, is for transient radiative cooling by a black region that is always at uniform temperature, and thus this curve starts at unity. Since the instantaneous emission from a black square at uniform temperature is $4b\sigma T_m^4(\tau)$, the black curve is also the ratio $T_m^4(\tau)/T_i^4$.

For clarity, some of the curves in Fig. 5 are shown dashed. For $B_0 = 1$, the region is optically too thin to radiate well. The radiative loss increases as B_0 increases to 2 and to 4. For $B_0 = 7$, the radiative loss begins at a somewhat higher value than for $B_0 = 4$ but then decreases below the $B_0 = 4$ values during the transient. For $B_0 = 15$, the region has become optically too thick to radiate well during the transient. The radiation is high for only a short initial period when the region is essentially at uniform temperature (logarithmic $\tilde{\tau}$ is used to show the early time behavior). It is interesting that, for large times, the curves for all B_0 tend to come fairly close together.

The transient decrease in mean temperature is in Fig. 6. Since the curves are normalized by the initial temperature, they all begin at unity. Figure 6a has a logarithmic abscissa to provide more detail at early times, and for clarity some curves are dashed. The curve for black radiation from a region at uniform temperature [Eq. (10) with $\epsilon_{ut} = 1$ and $A_R = 1$] is shown for comparison; this provides the most rapid temperature decrease. The curves extend to when 35% of the original energy has been lost. For $B_0 = 1$, the region is too thin to radiate well, and the time required to lose this amount of energy is about 75% longer than for a black region. The best cooling performance is for $B_0 \approx 4$, where the time is only about 25% longer than for blackbody radiation. For $B_0 = 15$, the region is too thick to radiate well from its interior, and this B_0 yields the longest cooling time.

Figure 6b provides $T_m(\tau)$ on a linear time scale to show the rapid temperature decrease at early times. The solid curves are the transient numerical solution. The dashed curves shown for comparison are computed from Eq. (10). This equation assumes the region is at uniform temperature at any time, and the emittance ϵ_{ut} for a uniform temperature region is used throughout cooling. For a specific B_0, the difference between the solid and dashed curves shows the effect of the nonuniform temperature distribution during the transient. The relatively cool transient temperatures near the boundary pro-

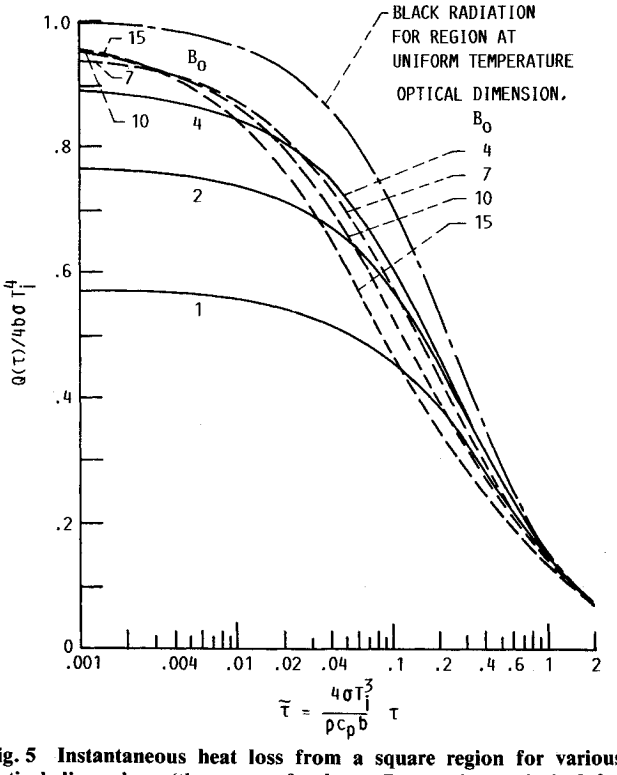

Fig. 5 Instantaneous heat loss from a square region for various optical dimensions (the curves for large B_0 are shown dashed for clarity).

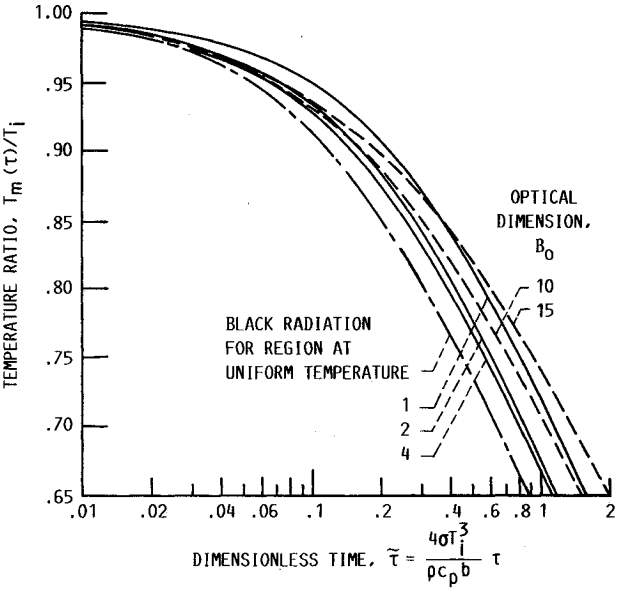

a) Cooling for various $B_0 = ab$ (curves for large B_0 are shown dashed for clarity)

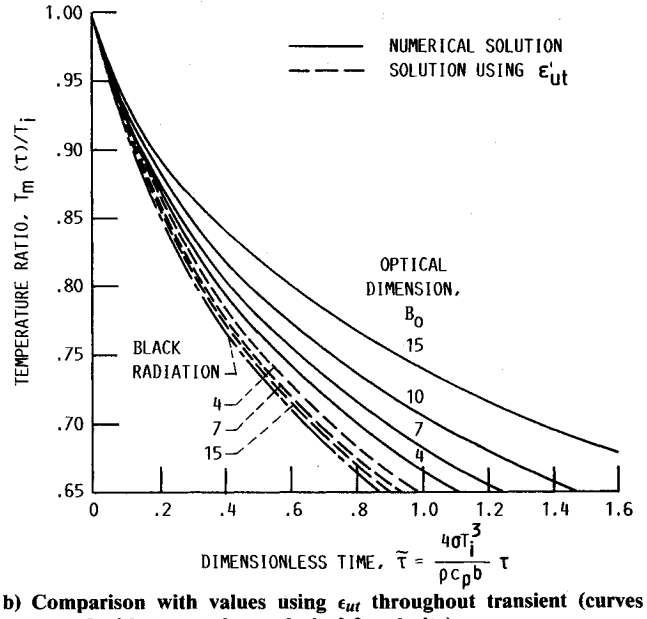

b) Comparison with values using ϵ_{ut} throughout transient (curves computed with ϵ_{ut} are shown dashed for clarity)

Fig. 6 Mean temperature variation during radiative cooling of a square region.

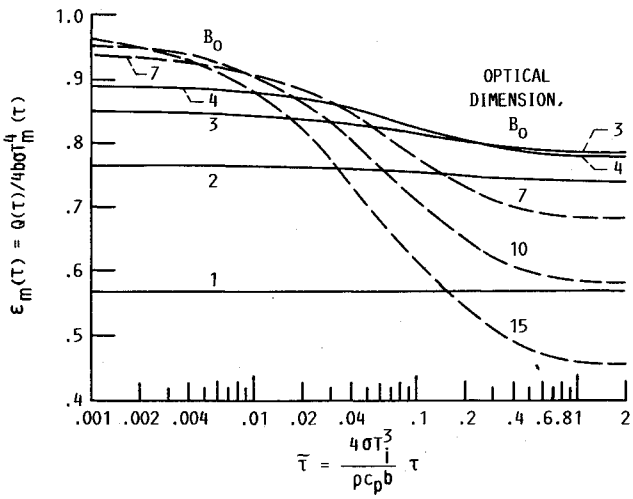

Fig. 7 Transient emittance for a square medium, based on instantaneous heat loss and instantaneous mean temperature.

duce a much lower cooling rate than for a region at uniform temperature.

The cooling behavior is also shown by the variation of the instantaneous emittance during the transient. The $\epsilon_m(\tau)$ for various B_0 are in Fig. 7; the $\epsilon_m(\tau)$ is based on the instantaneous $T_m^4(\tau)$ of the region. The theory in Ref. 5 for the cooling situation analyzed here shows that the $\epsilon_m(\tau)$ for each B_0 becomes constant as the transient temperature distribution moves toward a fully developed shape. This behavior is obtained in the transient numerical solution. The times where the curves become horizontal on Fig. 7 correspond in Fig. 6 to where $\tilde{T}_m \approx 0.75$. Hence the transient cooling must dissipate about 25% of the initial energy to establish the fully developed temperature profiles.

For small B_0 the temperature profiles are fairly flat, and the $\epsilon_m(\tau)$ in Fig. 7 remains fairly constant throughout the transient. For very short times, when the region is still close to being at uniform temperature, the $\epsilon_m(\tau)$ increases continuously with optical dimension B_0, as would be expected. For large times, where the temperature distributions have become nonuniform, the $\epsilon_m(\tau)$ increases with B_0 for B_0 up to about 3 and then decreases for larger B_0. This is a result of the relatively low transient temperatures that develop near the boundaries, thus yielding decreased radiative performance.

Conclusions

A transient numerical solution was carried out for the temperature distributions and radiative performance during cooling of a two-dimensional square radiating medium. At each time increment, the local radiative source term within the medium was evaluated from the temperature distribution by Gaussian integration over rectangular subregions. The results for local radiative heat fluxes along the boundary, and overall emittance of the region, agreed very well with available limiting cases. The comparisons indicate that the numerical technique provided an excellent approximation to the exact solution. The situation analyzed was for radiation into black surroundings at a much lower temperature than that of the radiating medium. For this condition, a previous similarity analysis had indicated that the transient solution reaches an equilibrium where the overall heat loss and the mean temperature to the fourth power are both changing at the same rate with time. This behavior was obtained in the transient numerical solution, and it yields a constant emittance of the region for the remainder of the transient. It was found that this constant emittance, which is a function of optical dimension, was reached after approximately 25% of the original energy had been radiated away. The transient radiative ability of the region depends on its optical thickness. An optically thin region does not radiate well. When the region is optically thick, the energy cannot propagate easily to the boundaries, and during transient cooling the regions near the boundaries are much cooler than the interior. This produces a reduced radiative ability if the region is too thick. It was found that a square region with an optical side length of about 4 provided the highest average level of emittance throughout the cooling transient.

Acknowledgment

Frank Molls of NASA Lewis Research Center provided considerable help in developing the computer program. His helpful discussions on numerical methods are also gratefully acknowledged.

References

[1]Fiveland, W. A., "Discrete-Ordinates Solutions of the Radiative Transport Equation for Rectangular Enclosures," *Journal of Heat Transfer,* Vol. 106, No. 4, Nov. 1984, pp. 699–706.

[2]Truelove, J. S., "Discrete-Ordinate Solutions of the Radiation Transport Equation," *Journal of Heat Transfer,* Vol. 109, No. 4, Nov. 1987, pp. 1048–1051.

[3]Razzaque, M. M., Klein, D. E., and Howell, J. R., "Finite Element Solution of Radiative Heat Transfer in a Two-Dimensional Rectangular Enclosure With Gray Participating Media," *Journal of Heat Transfer,* Vol. 105, No. 4, Nov. 1983, pp. 933–936.

[4]Razzaque, M. M., Howell, J. R., and Klein, D. E., "Coupled Radiative and Conductive Heat Transfer in a Two-Dimensional Rectangular Enclosure with Gray Participating Media Using Finite Elements," *Journal of Heat Transfer,* Vol. 106, No. 3, Aug. 1984, pp. 613–619.

[5]Siegel, R., "Some Aspects of Transient Cooling of a Radiating Rectangular Medium," *International Journal of Heat and Mass Transfer,* Vol. 32, No. 10, 1989, pp. 1955–1966.

[6]Yuen, W. W., and Wong, L. W., "Analysis of Radiative Equilibrium in a Rectangular Enclosure With Gray Medium," *Journal of Heat Transfer,* Vol. 106, No. 2, May 1984, pp. 433–440.

[7]Yuen, W. W., and Ho, C. F., "Analysis of Two-Dimensional Radiative Heat Transfer in a Gray Medium With Internal Heat Generation," *International Journal of Heat and Mass Transfer,* Vol. 28, No. 1, 1985, pp. 17–23.

[8]Yuen, W. W., and Takara, E. E., "Analysis of Combined Conductive-Radiative Heat Transfer in a Two-Dimensional Rectangular Enclosure with a Gray Medium," *Journal of Heat Transfer,* Vol. 110, No. 2, May 1988, pp. 468–474.

[9]Ho, C. H., and Ozisik, M. N., "Combined Conduction and Radiation in a Two-Dimensional Rectangular Enclosure," *Numerical Heat Transfer,* Vol. 13, No. 2, 1988, pp. 229–239.

[10]Yuen, W. W., and Wong, L. W., "Numerical Computation of an Important Integral Function in Two-Dimensional Radiative Transfer," *Journal of Quantitative Spectroscopy and Radiative Transfer,* Vol. 29, No. 2, 1983, pp. 145–149.

[11]Siegel, R., "Analytical Solution for Boundary Heat Fluxes from a Radiating Rectangular Medium," *Journal of Heat Transfer,* Vol. 113, No. 1, 1991, pp. 258–261.

[12]Goldstein, C. M., "Numerical Integration by Gaussian Quadrature," NASA TMX-52008, March 1965.